Published in final edited form as:

Mol Oral Microbiol. 2017 August ; 32(4): 341–353. doi:10.1111/omi.12176.

In vitro characterization of biofilms formed by *Kingella kingae*

Jeffrey B. Kaplan[1], **Vandana Sampathkumar**[2], **Meriem Bendaoud**[2], **Alexander K. Giannakakis**[3], **Edward T. Lally**[3], and **Nataliya V. Balashova**[3,*]

[1]Department of Biology, American University, Washington, DC 20016

[2]Department of Oral Biology, Rutgers School of Dental Medicine, Rutgers University, Newark, NJ 07103

[3]Department of Pathology, School of Dental Medicine, University of Pennsylvania, Philadelphia, PA 19104

Summary

The Gram-negative bacterium *Kingella kingae* is part of the normal oropharyngeal mucosal flora of children under four years old. *K. kingae* can enter the submucosa and cause infections of the skeletal system in children including septic arthritis and osteomyelitis. The organism is also associated with infective endocarditis in children and adults. Although biofilm formation has been coupled with pharyngeal colonization, osteoarticular infections, and infective endocarditis, no studies have investigated biofilm formation in *K. kingae*. In this study we measured biofilm formation by 79 *K. kingae* clinical isolates using a 96-well microtiter plate crystal violet binding assay. We found that 37/79 strains (47%) formed biofilms. All strains that formed biofilms produced corroding colonies on agar. Biofilm formation was inhibited by proteinase K and DNase I. DNase I also caused the detachment of pre-formed *K. kingae* biofilm colonies. A mutant strain carrying a deletion of the pilus gene cluster *pilA1pilA2fimB* did not produce corroding colonies on agar, autoaggregate in broth, or form biofilms. Biofilm forming strains have higher level of *pilA1* expression. The extracellular components of biofilms contained 490 μg/cm^2 of protein, 0.68 μg/cm^2 of DNA, and 0.4 μg/cm^2 of total carbohydrates. We concluded that biofilm formation is common among *K. kingae* clinical isolates, and that biofilm formation is dependent on the production of proteinaceous pili and extracellular DNA. Biofilm development may have relevance to the colonization, transmission, and pathogenesis of this bacterium. Extracellular DNA production by *K. kingae* may facilitate horizontal gene transfer within the oral microbial community.

Introduction

Kingella kingae is a Gram-negative coccobacillus that asymptomatically colonizes the oropharynx of up to 30% of children 6–36 months old (Yagupsky, 2015). It is believed that damage of the respiratory and buccal epithelium allows the bacterium to enter the bloodstream and to seed in distant organs of the body. This can lead to osteoarticular

*Address correspondence to: Nataliya Balashova, Department of Pathology, University of Pennsylvania, School of Dental Medicine, 240 S. 40th St., 316 Levy Building, Philadelphia, PA 19104, USA. Tel.: (215) 898-5073; Fax: (215) 898-2050. natbal@upenn.edu.

infections including septic arthritis, osteomyelitis, bacteremia, and infective endocarditis. Due to improved detection methods, there has been an increasing number of invasive *K. kingae* infections cases identified in recent years. The organism is now considered the leading cause of skeletal infections in young children (Chometon *et al.*, 2007; Gene *et al.*, 2004; Ilharreborde *et al.*, 2009). *K. kingae* osteomyelitis and septic arthritis usually have a good prognosis when treated with antibiotics, however onset of these infections is generally insidious, and the disease is frequently diagnosed with considerable delay (Yagupsky, 2015). Infective endocarditis caused by *K. kingae* has been diagnosed in otherwise healthy children or adult patients and was associated with significant morbidity and mortality (Foster and Walls, 2014).

Several *K. kingae* virulence factors have been identified. The organism produces potent RTX toxin with broad cellular specificity that plays the key role in the organism virulence (Chang *et al.*, 2014; Kehl-Fie and St Geme, 2007). *K. kingae* releases RtxA-bound outer membrane vesicles (OMVs) that exhibit hemolytic and leukotoxic activity (Maldonado *et al.*, 2011). *K. kingae* produces at least two different types of adhesive pili that mediate binding of bacterial cells to respiratory epithelial cells and synovial cells (Kehl-Fie *et al.*, 2008). However, the mechanisms by which *K. kingae* colonizes the oropharynx, disperses to the submucosa, and causes systemic diseases are still unclear.

Adherent communities of bacteria known as biofilms play a role in the pathogenesis of many chronic infections including osteoarticular infections (Lynch and Robertson, 2008) and infective endocarditis (Parsek and Singh, 2003). Biofilms enable bacteria to colonize surfaces and evade the host immune system. However, few studies have investigated biofilm formation in *K. kingae*. Bendaoud et al. (Bendaoud *et al.*, 2011) showed that one strain of *K. kingae* (strain PYKK181) formed biofilms in polystyrene microtiter plate wells, and that biofilm formation was inhibited by a self-synthesized galactofuranose-containing exopolysaccharide named PAM galactan. *K. kingae* PAM galactan is one of a growing number of bacterial exopolysaccharides that exhibit broad-spectrum nonbiocidal antibiofilm activity (Rendueles *et al.*, 2013). No additional studies on *K. kingae* biofilm formation have been reported.

The purpose of the present study was to characterize *K. kingae* biofilms and measure biofilm formation in a larger collection of *K. kingae* clinical isolates. We analyzed a total of 79 strains that included strains isolated from patients with bacteremia, infective endocarditis, osteomyelitis and septic arthritis; strains isolated from healthy subjects; and *K. kingae* type strain ATCC 23330. Here we report our findings on the prevalence and mechanism of biofilm formation among *K. kingae* clinical isolates.

Methods

Bacterial strains, media and growth conditions

The *K. kingae* strains utilized in this study were described previously (Banerjee *et al.*, 2013) and are listed in Table 1S (Supplementary data). The identification of all strains was confirmed by 16S rRNA gene sequence analysis. Liquid growth medium (designated TSB+ broth) consisted of filter-sterilized Tryptic soy broth supplemented with 6 g L^{-1} yeast

extract, 8 g L^{-1} glucose and 4 g L^{-1} sodium bicarbonate. Solid media (designated TSA agar) were further supplemented with 1.5 g L^{-1} agar. Unless otherwise indicated, all cultures were incubated statically at 37°C in a 10% CO_2 atmosphere.

Biofilm assay

Staining the biofilms was performed by crystal violet assay (Izano *et al.*, 2008; Merritt *et al.*, 2005). Several loopfuls of *K. kingae* cells were transferred from a 24-h-old TSA agar plate to a 1.5-mL microcentrifuge tube containing 500 μL of fresh TSB+ broth. Cells were dispersed by vortex agitation and the A_{490} of the cell suspension was adjusted to 1.0 with TSB+ broth. Cells were dilute 1:100 in fresh TSB+ broth and aliquots of cells (200 μL each, ca. 10^4–10^5 cfu mL^{-1}) were transferred to the wells of a 96-well polystyrene microtiter plate (Falcon No. 353936 or Corning No. 2592). After incubation for 24 h, wells were rinsed with water to remove loosely adherent cells and then stained for 1 min with 200 μL of Gram's crystal violet. Wells were then rinsed with water and dried. The amount of biofilm biomass was quantitated by distaining the wells with 200 μL of 33% acetic acid and measuring the absorbance of the crystal violet solution in a microplate spectrophotometer set at 595 nm.

Biofilm inhibition assay

Bacterial inocula were prepared and diluted 1:100 in fresh TSB+ broth as described in "Biofilm assay" Section. Inocula were supplemented with 10 μg mL^{-1} proteinase K (Sigma-Aldrich) or 10 μg mL^{-1} recombinant human DNase I (Genentech). Aliquots of inocula were transferred to microtiter plate wells, incubated for 24 h, and biofilm formation was quantitated by crystal violet staining.

Biofilm detachment assay

Biofilms detachment assay was described previously (Izano *et al.*, 2008). *K. kingae* biofilms were cultured in microtiter plate wells for 24 h as described in "*Biofilm assay*" section. Wells were rinsed with water to remove loosely adherent cells. Wells were then filled with 200 μL of 10 μg mL^{-1} proteinase K in water, or 10 μg mL^{-1} DNase I in 150 mM NaCl, 1 mM $CaCl_2$. Control wells were filled 200 μL of vehicle alone. After 1 h at 37°C, wells were rinsed with water to remove loosely adherent cells and biofilm was quantitated by crystal violet staining.

Autoaggregation assay

Bacterial inocula were prepared and diluted to an A_{490} of 1.0 in fresh TSB+ broth as described in "Biofilm assay" Section. Cells were resuspended by vortex agitation and the tubes were then incubated statically for 10 min and photographed.

Mutagenesis Construction of mutagenic plasmid

A plasmid used to delete the *K. kingae pilA1pilA2fimB* gene cluster (designated plasmid pVS5) was constructed as follows. First, the DNA sequence upstream of *pilA1* was amplified from *K. kingae* strain PYKK109 using PCR primers RecF and RecPstR (Table 2S, Supplementary data). The PCR product (1.6 kb) was digested with *Pst*I and ligated into the *Pst*I site of plasmid pGEM-T Easy (Promega). The resulting plasmid was designated pVS1.

Next, the region downstream of *fimB* was amplified from *K. kingae* strain PYKK109 using PCR primers tRNAAatF and tRNAR. The PCR product (1.2 kb) was ligated into the single 3´-T overhangs located in the polylinker of pGEM-T Easy. The resulting plasmid (designated pVS2) was digested with *Aat*II and *Eco*RI to release the ligated fragment, which was then ligated into the *Aat*II/*Eco*RI sites of pVS1. The resulting plasmid was designated pVS4. Next, the *aphA3* kanamycin resistance gene was amplified from plasmid pFalcon2 (Sheets *et al.*, 2008) using PCR primers KmF and KmR. The PCR product (1.0 kb) was ligated into the single 3´-T overhangs in pGEMT-Easy, resulting in plasmid pVS3. Finally, mutagenic plasmid pVS5 was constructed by ligating the *aphA3* kanamycin resistance gene released by *Eco*RI digestion of plasmid pVS3 into *Eco*RI digested pVS4. All plasmid constructs were confirmed by DNA sequence analysis.

Bacterial transformation

Transformation of *K. kingae* was performed as described previously (Kehl-Fie and St Geme, 2007). *K. kingae* strain PYKK109 was cultured overnight on TSA agar and resuspended to an A_{600} of 0.8 in TSB+ broth containing 2% fetal bovine serum. A volume of 100 μL of the cell suspension was transferred to a microcentrifuge tube and 5 μL of 10 mM $CaCl_2$ and 5 μL (1 μg) of plasmid pVS5 DNA were added. The mixture was incubated at room temperature for 30 min. An equal volume of TSB+ broth containing 4% horse serum was added, and the cells were incubated at 37°C for 2 h. The cells were then plated onto TSA agar containing 25 μg mL^{-1} kanamycin to select for transformants. Genomic DNA was isolated from the transformants using a QIAamp DNA Mini Kit (Qiagen). PCR primers pilAF and fimBR (Table 1), which hybridize to sequences that flank the homologous regions, were used to confirm integration of *aphA3* in transformants for the *pilA1pilA2fimB* mutant strain, which was designated strain VS1001. The orientation of the *aphA3* kanamycin cassette was confirmed using PCR primers KmF1 and Kk58piliR.

Real-time quantitative reverse transcription PCR (RT-qPCR)

K. kingae strains were grown on plates for 18 h, bacterial mass was collected. Total RNA from the bacterial cells was extracted with 1 ml preheated to 65°C Tri Reagent (Sigma) and isolated according to the Tri Reagent manufacture's protocol. To remove residual DNA, the RNA samples were treated with RQ1 DNase (Fisher Scientific). The DNase was inactivated by heating at 65°C for 10 min. Then RNA samples were additionally purified using an RNeasy Mini kit and the lipid-rich tissue protocol (Qiagen). To create cDNA, 2 μg of RNA, random hexamers, and SuperScript II were used according to the manufacturer's instructions (Invitrogen). Quantitative real-time PCR was carried out in an Applied Biosystems™ 7300 real-time PCR platforms (Thermo Fisher Scientific) by using the Power SYBR Green PCR Master Mix (Thermo Fisher Scientific) and primers presented in Table 2S, Supplementary data. The PCR amplification was carried out in a total volume of 46 μl, containing 44 μl of 2 SYBR green PCR master mix, approximately 25 ng of the cDNA sample, and 200 nM each primer. The reaction conditions were 95°C for 3 min followed by 32 cycles of 95°C for 15 s, 61°C for 20 s, and 72°C for 30 s; this was followed by a final 72°C for 3 min. All reactions were run in triplicate; the assay was performed three independent times. The expression of the genes was analyzed using the software provided by Applied Biosystems™. The second

derivative maximum of the slope of the amplification curves was used as Ct (cycle threshold) values.

Biofilm biochemical analysis

The quantitative biochemical analysis of biofilms was performed as previously described (Wu and Xi, 2009), with some modifications. Briefly, biofilms were formed in ten 100 mm cell culture polystyrene dishes (FisherScientific No.10810274) by incubating 20 mL of TSB + broth with 1:100 10^4–10^5 cfu mL^{-1} *K. kingae* at 37 °C in 5% CO_2 environment for 24 h. The biofilm in each plate was gently washed twice with deionized water, then the biofilm mass removed with a cell scraper and placed in 5 mL of 0.9% NaCl. Samples from the plates were pooled and the biofilm suspension was homogenized by vortexing for 2 min. The resulting mixture was divided into two parts. Half of the solution was passed through a 0.2 μm PES filter (Millex, EMD Millipore) to separate extracellular components of *K. kingae* biofilms.

Protein content of *K. kingae* biofilms was quantified by a bicinchoninic acid (BCA) assay (Pierce). The absorbance at 562 nm was determined using bovine serum albumin (BSA) standard curve as a reference to estimate the protein concentration in the sample.

Total carbohydrates were quantified by a phenol-sulfuric acid colorimetric assay using Total carbohydrate Assay Kit (BioVision) kit according to the manufacturer instructions. The absorbance at 490 nm was determined and compared to a glucose standard curve to estimate the mass of carbohydrates in the sample.

DNA content was quantified using SYTOX® Green Nucleic Acid Stain (Life Technologies) as described previously (Ravaioli *et al.*, 2011) with modifications. Briefly, 200 μL of the biofilms extracellular matrix solution were mixed with 100 μL of 5 μM buffered Sytox solution in 96-well plate wells, and the plate was incubated in the dark at 37 °C for 40min. Fluorescence was read at an emission wavelength of 520 nm and total DNA estimated by extrapolation from a standard curve using Lambda DNA (New England Biolabs). Treatment of biofilms with the broad spectrum micrococcal nuclease (New England Biolabs) was performed for 1 h at 37 °C.

Fluorescent microscopy

Bacterial inocula were prepared and diluted 1:100 in fresh TSB+ broth as in “Biofilm assay” Section. Aliquots of diluted cells (250 μL each) were pipetted onto the surface of sterile glass slides, and the slides were placed inside a Petri dish. After incubation for 24 h, the slides were rinsed with water and stained with SYTO9 (Molecular Probes) for 20 min in the dark. Slides were then rinsed with water to remove excess stain. Biofilm bacteria were visualized at 10 × magnification using a Nikon Eclipse 80i fluorescent microscope. Extracellular DNA production in bacterial cultures grown in ibiTreat 60 μ-dishes (Ibidi) was examined using a Nikon A1R laser scanning confocal microscope with a 60× water objective (NA 1.2) after staining with 5 μM SYTOX® Green Nucleic Acid Stain (Life Technologies) for 15 min. The images were processed using Nikon's elements software 4.1 (Nikon).

Atomic force microscopy (AFM)

The bacteria were grown for 24 h on TSA agar. The colonies were washed off the agar pates with distilled water and dried for 15 min. AFM samples were prepared by mounting of agar pieces on glass slides. AFM images were obtained using Asylum MFP-3D (Oxford Instruments) operated in tapping mode (scan rate = 0.3–0.4 Hz, Si tip, probe stiffness ~40 N/m, drive frequency 316 kHz, ambient temperature). Electronic spectra were recorded on a Varian 5000 UV/vis/NIR instrument. The relative peak positions were assigned via spectral deconvolution using Origin 7.5 software (Originlab). Samples were interrogated in 2 mm path-length fused-silica cells under argon.

Statistics and reproducibility of results

All crystal violet binding assays were carried out in duplicate wells, which exhibited an average variation in absorbance values of 7%. All assays were repeated two or more times and in all cases the observed patterns of biofilm formation, inhibition and detachment were reproducible. The data were analyzed using a Student's *t*-test, with $P < 0.05$ considered to be statistically significant. The analysis was performed using SigmaPlot version 11.0 software (Systat Software).

Results

Biofilm formation by K. kingae clinical isolates

A total of 79 *K. kingae* strains were tested for biofilm formation using a 96-well microtiter plate crystal violet binding assay (Table 1S, Supplementary data). The test strains included 28 strains isolated from bacteremia patients, 25 from septic arthritis patients, 19 from healthy subjects, 6 from osteomyelitis patients, and 1 from an infective endocarditis patient. The strains were collected in five locations on three continents.

Figure 1 shows the average amount of biofilm formation by each of the 79 test strains. Strains that produced a depression or pit in the agar on which they were grown were designated “corroding” (Kehl-Fie *et al.*, 2010). A total of 58/79 strains (66%) were corroding. Corroding strains formed more biofilm than noncorroding strains ($P < 0.001$). Overall, 47% of all strains and 47% of corroding strains formed biofilms using an A_{595} value of 0.2 as a cutoff ($P < 0.001$ compared to the background A_{595} value of 0.05). Eleven strains (KKC2005004457, KKM2003000180 (USA); PYKK109, PYKK133, PYKK135, PYKK143 and PYKK181 (Israel); 9911+17199, 0111+28183, 0601+26281, and 0401+20177 (Iceland)) produced biofilms that resulted in A_{595} values >1.0 in the crystal violet binding assay. Figure 2 shows representative colony morphologies on agar and biofilm phenotypes in broth for corroding strain PYKK109 and noncorroding strain ATCC 23330. Strain PYKK109, like all other biofilm forming *K. kingae* strains, produced biofilms both on the bottom of the microtiter plate well and along the side of the well at the air/liquid interface. Strain PYKK143 also formed a floating pellicle on the surface of the broth.

Preliminary studies in our laboratory suggest that the corroding and biofilm phenotypes can be lost upon repeated subculture on TSA agar or in TSB+ broth. For instance, after 5 passages of PYKK109 on TSA agar the amount of biofilms identified by crystal violet

binding assay decreased from A_{595}=1.1±0.06 to A_{595}= 0.7±0.03. In support of this hypothesis we observed that Icelandic isolates (9911+17199, 0111+28183, 0601+26281, and 0401+20177), which were comparatively less used in laboratory studies, formed the strongest biofilms that resulted in A_{595} ≥1.3 by crystal violet binding assay.

Biofilm composition

We selected strain PYKK109 to characterize the biochemical composition of the biofilms. We quantitated the amount of DNA, carbohydrates, and proteins in the total biofilm and its extracellularly secreted components as described in "*Biofilm biochemical analysis*" section. About 95% of formed biofilms, as was quantified by the remaining biofilm measurement with crystal violet, were collected by scraping from polystyrene plates without additional chemical treatment. The extracellular biofilm's fraction was separated by filtration through 0.22 μm filter and the composition of total biofilms and biofilms extracellular matrix was identified. Protein content was measured with a BCA assay, and was present extracellularly at a concentration 490 ± 0.55 μg/cm^2. Applying a total carbohydrate phenol-sulfuric acid method, which can detect most forms of carbohydrates, we identified 0.4 ± 0.05 μg/cm^2 of total carbohydrates in the extracellular constituents. Extracellular DNA was detected at 0.68 ± 0.08 μg per cm^2. To verify that the fluorescence was from extracellular biofilm matrix and not from DNA within bacterial cells, damaged during biofilms collection procedure, a separate set of biofilms were incubated with the broad spectrum micrococcal nuclease (Kiedrowski *et al.*, 2011). Pre-treatment of total biofilms with micrococal nuclease caused 92% reduction in extracellular DNA suggesting that extracellular DNA present in PYKK109 biofilms. The summarized data are presented in Table 1. Extracellular DNA production was characteristic feature of biofilm-forming strains and was visualized by fluorescent microscopy after staining of bacterial cultures with SYTOX® Green Nucleic Acid Stain. Figure 3 demonstrates extracellular DNA production by PYKK109 but not strain ATCC 23330.

Biofilm formation is mediated by proteinaceous adhesins and extracellular DNA

To investigate the mechanism of *K. kingae* biofilm formation, we measured the effect of two enzymes, Proteinase K and DNase I, on biofilm formation by strain PYKK109. Figure 4 (left-hand graph) shows that both enzymes significantly inhibited biofilm formation. Both the bottom biofilm and the air/liquid biofilm were inhibited. Proteinase K and DNase I also inhibited both bottom and air/liquid biofilm formation by strains KKC2005004457 and PYKK143 (data not shown). Neither enzyme affected the growth rate of *K. kingae.*

We then measured the ability of proteinase K and DNase I to detach pre-formed 24-h-old *K. kingae* PYKK109 biofilms. DNase I, but not proteinase K, caused significant detachment of the biofilms (Fig. 4, right-hand graph). Both the bottom and air/liquid biofilms were detached. DNase I, but not proteinase K, also efficiently detached pre-formed 24-h-old bottom and air/liquid biofilms produced by strains KKC2005004457 and PYKK143.

A pilus mutant strain is deficient in biofilm formation

K. kingae produces adhesive type IV pili that are essential for mediating adherence to respiratory epithelial and synovial cells (Kehl-Fie *et al.*, 2008). We found that the

pilA1pilA2fimB region of the chromosome was conserved among five *K. kingae* biofilm forming strains (269–492 (Kehl-Fie and St Geme, 2007), PYKK081 (Kaplan *et al.*, 2012), PYKK109, PYKK121 and PYYY181) and three noncorroding strains non-biofilm forming strains (ATCC 23330, PYKK102 and PYKK190) as determined by PCR and DNA sequence analysis (Figure 1S). To determine whether pili play a role in *K. kingae* biofilm formation, we constructed a mutant strain that carried a deletion of the *pilA1pilA2fimB* gene cluster, which encodes two type IV pilus subunit proteins and a pilus accessory protein (Kehl-Fie *et al.*, 2008). The mutant strain (designated strain VS1001; Fig. 1S, Supplementary data) was constructed in background strain PYKK109. Strain VS1001 exhibited the same growth rate as strain PYKK109 but produced noncorroding colonies on agar (data not shown). In the microtiter plate assay, strain VS1001 exhibited significantly less crystal violet binding than strain PYKK109 (A_{595} = 0.02 ± 0.00 for VS1001 versus 1.99 ± 0.05 for PYKK109; $P <$ 0.01). Strain VS1001 was also deficient in autoaggregation in broth (Fig. 5A), biofilm formation on glass slides (Fig. 5B), and agar corrosion (Fig. 5C).

Biofilm forming strains have elevated levels of pilA1 transcripts

To assess whether there is the correlation between pilus expression with the ability of *K. kingae* strains to form biofilms we quantified the *pilA1, pilA2, and fimB* transcripts levels in corroding biofilm forming strains PYKK109, 0211+12480, noncorroding biofilm forming strain PYKK081, and noncorroding, non-biofilm forming strains ATCC 23330, 0604+15110 using RT-qPCR analysis. This analysis revealed that biofilm producing strains have higher level of *pilA1* transcripts suggesting that the gene is highly expressed in biofilm forming strains. For example the level of *pilA1* transcript inPYKK109 was 80 fold more than that in the strain ATCC 23330) (Figure 6). The difference in expression *pilA2* and *fimB* was less pronounced or not significant. Importantly, while strain ATCC 23330 has low level of expression of all three pilus genes, another non-biofilm forming strain 0604+15110 has low expression of *pilA1* indicating that the expression of the major pilus subunit is the most critical for biofilm formation.

Discussion

In the present study we used a crystal violet binding assay and fluorescent microscopy to demonstrate that clinical isolates of *K. kingae* are capable of forming biofilms in polystyrene microtiter plates and on glass slides. In microtiter plates, biofilm formation occurred both on the bottom of the well and along the side of the well at the air/liquid interface. One strain formed a floating pellicle on the surface of the broth. All of these phenotypes are exhibited by other species of biofilm-forming bacteria (Kaplan and Mulks, 2005; Marti *et al.*, 2011).

We also used two biofilm matrix-degrading enzymes to investigate the composition of the *K. kingae* extracellular biofilm matrix. We found that formation of both the bottom and air/liquid interface biofilms was inhibited by proteinase K and DNase I, suggesting that both biofilms produce a biofilm matrix containing proteinaceous adhesins and extracellular DNA. Since mature biofilms were efficiently detached by DNase I but not by proteinase K, it is possible that both proteinaceous adhesins and extracellular DNA play a role in the initial stages of *K. kingae* biofilm formation, but that extracellular DNA is a major intercellular

adhesin in mature biofilms. Previous studies showed that several other bacteria produce biofilms that are resistant to removal by proteolytic enzymes (Lequette *et al.*, 2010).

The extracellular DNA and proteins were major biofilms matrix components of PYKK109 biofilms. Extracellular DNA is a biofilm matrix component in many different species of bacteria (Montanaro *et al.*, 2011) including members of Neisseriaceae family *Neisseria gonorrhoeae* (Steichen *et al.*, 2011) and *Neisseria meningitides* (Lappann *et al.*, 2010). It was found to play an essential role in biofilm formation and support of its integrity on hard and soft tissues in oral cavity (Jakubovics and Grant Burgess, 2015). Several mechanisms of extracellular DNA accumulation exist. In *N. meningitides* the release of extracellular DNA can be mediated by lytic transglycosydases and cytoplasmic N-acetylmuramyl-L-alanine amidase as well as autolytic activity of outer membrane phospholipase A (Lappann *et al.*, 2010). DNA could accumulate from passive death of cells followed by cell lysis. Indeed, lifespan of *K. kingae* colonies on blood agar plates do not exceed 48 h at 37 °C. In a wide range of bacteria *cidAB* and *lrgAB* genes encode holin/antiholin proteins that regulate DNA release and biofilm formation (Bayles, 2007). The genomes of *K. kingae* strains ATCC 23330 (GenBank Accession number AFHS01000000) and PYKK081 (GenBank Accession number AJGB00000000) both contain homologues of the *lrgAB* gene clusters, which may perform similar biofilm-related functions in *K. kingae*. In addition to *K. kingae* produces several nucleases, that may play a role in the biofilm formation and remodeling, as it was demonstrated for *N. gonorrhoeae* termonuclease Nuc (Steichen *et al.*, 2011). *K. kingae* genes potentially involved in extracellular DNA accumulation are presented in Table 3S.

One of mechanisms of DNA biofilm matrix creation is secretion of OMVs loaded with DNA. We have found that OMVs sample the isolated from *K. kingae* strain PYKK081 contained 0.5 mg/ml DNA (Maldonado *et al.*, 2011). Interestingly, biofilm producers PYKK081, PYKK189, PYKK135 were reported to release higher amount of OMVs per g of bacterial biomass (average 0.07±0.003 mg) than non-biofilm producing strains ATCC 23330, PYKK190, PYKK101 (average 0.02±0.002 mg) (Maldonado *et al.*, 2011). It is worth noting *K. kingae* is naturally transformable organism and it is likely that uptake of extracellular DNA facilitate the spread of genes through horizontal transfer (Frye *et al.*, 2013).

Corroding or pitting of the agar surface is a phenotype exhibited by Gram-negative and Gram-positive bacteria that colonize the respiratory tract (Henriksen, 1974), suggesting that it could be a useful factor for establishing an ecological niche of colonization on mucos membranes. Previous studies showed that corrosion of agar surfaces correlates with the production of type IV pili in some bacteria (Azakami *et al.*, 2005; Kraus and Glassman, 1974; Kyme *et al.*, 2003). Type IV pili have also been associated with autoaggregation and biofilm formation in many bacteria (Kachlany *et al.*, 2001; Yi *et al.*, 2004). Consistent with these results, we found that *K. kingae* mutant strain VS1001 (Δ*pilA1pilA2fimB*) produced noncorroding colonies on agar and was deficient in autoaggregation and biofilm formation in broth. Since *pilA1* encodes the major *K. kingae* type IV pilus subunit protein (Kehl-Fie and St Geme, 2007), these results suggest that type IV pili may mediate agar corrosion, autoaggregation and biofilm formation in *K. kingae*.

We found that *K. kingae* biofilm formation correlated with a corroding phenotype on agar, nevertheless 47% of corroding strains do not form biofilms. Kehl-Fie et al. (Kehl-Fie *et al.*, 2010) reported that *K. kingae* clinical isolates exhibit various colony morphologies on chocolate agar including "nonspreading/noncorroding," "spreading/corroding" and "domed." Although we readily detected the corroding and noncorroding colony morphologies on the TSA agar plates utilized in our study, we did not observe the spreading and nonspreading phenotypes even when using motility agar plates (unpublished data). It is possible that this spreading phenotype results from type IV pilus-mediated twitching motility (Mattick, 2002), and that twitching motility is up-regulated on chocolate agar or down-regulated on TSA agar. Kehl-Fie et al. (Kehl-Fie *et al.*, 2010) also showed that the amount of piliation varied among *K. kingae* clinical isolates. We found that the quantity of biofilm formation varied among *K. kingae* clinical isolates, so it is tempting to speculate that the level of piliation correlates with the level of biofilm formation in corroding strains. We found that the biofilm phenotype was exhibited by *K. kingae* strains that were reported to produce both low and high levels of type IV pili and the expression of *pilA1* is essential for biofilm formation.

We also observed no correlation between the clinical syndrome of the subject, the anatomical site from which the strain was isolated, or the pulse-filed gel electrophoresis clonal type exhibited by the strain (Amit *et al.*, 2012). Previous studies found that the regulation type IV pilus expression in *K. kingae* is complex and influenced by both the genetic regulators and environmental cues (Kehl-Fie *et al.*, 2009). It is possible that biofilm formation is common among *K. kingae* clinical isolates, but that the biofilm phenotype is lost upon repeated subculture in the laboratory (Fine *et al.*, 1999; Kaplan and Mulks, 2005), or that the biofilm and/or corroding phenotypes are selected against when *K. kingae* enters the bloodstream and disseminates to remote sites (Kehl-Fie *et al.*, 2010). *K. kingae* strains used in this study were received from different clinical laboratories and the number of passages performed with those strains was not controlled. Therefore, we believe that the variation in the amount of biofilms produced can be partly attributed to the domestication of the strains used in the study.

In summary, our results demonstrate that *K. kingae* clinical isolates produce biofilms *in vitro*. Since biofilms have been shown to play a role in colonization of mucosal surfaces and other tissues such as bone and heart valves in many bacteria (Brady *et al.*, 2008; Parsek and Singh, 2003; Shirtliff and Mader, 2002), we speculate that biofilm formation may have relevance to the colonization, transmission and pathogenesis of *K. kingae*.

Supplementary Material

Refer to Web version on PubMed Central for supplementary material.

Acknowledgments

The authors thank Pablo Yagupsky (Soroka University Medical Center, Beer-Sheva, Israel), Sharon Pendergrass (Minnesota Department of Health, St. Paul, MN), and Paul Planet (Children's Hospital of Philadelphia, Philadelphia, PA) for providing bacterial strains, as well as Joseph St. Geme 3rd and Eric Porsch (Children's Hospital of Philadelphia, Philadelphia, PA) for providing plasmid pFalcon2. The authors thank Elizabeth R. Hatfield and Sangho Kim for the technical assistance in this project. This work was supported in part by NIH grants

AI82392 (to J.B.K.) and R01DE009517 (to E.T.L.) as well as by AHA grant 9SDG2310194 and UPENN URF grant (to N.V.B.).

References

Amit U, Porat N, Basmaci R, et al. Genotyping of invasive Kingella kingae isolates reveals predominant clones and association with specific clinical syndromes. Clin Infect Dis. 2012; 55:1074–1079. [PubMed: 22806593]

Azakami H, Akimichi H, Usui M, Yumoto H, Ebisu S, Kato A. Isolation and characterization of a plasmid DNA from periodontopathogenic bacterium, Eikenella corrodens 1073, which affects pilus formation and colony morphology. Gene. 2005; 351:143–148. [PubMed: 15869847]

Banerjee A, Kaplan JB, Soherwardy A, et al. Characterization of TEM-1 beta-lactamase producing Kingella kingae clinical isolates. Antimicrob Agents Chemother. 2013

Bayles KW. The biological role of death and lysis in biofilm development. Nat Rev Microbiol. 2007; 5:721–726. [PubMed: 17694072]

Bendaoud M, Vinogradov E, Balashova NV, Kadouri DE, Kachlany SC, Kaplan JB. Broad-spectrum biofilm inhibition by Kingella kingae exopolysaccharide. J Bacteriol. 2011; 193:3879–3886. [PubMed: 21602333]

Brady RA, Leid JG, Calhoun JH, Costerton JW, Shirtliff ME. Osteomyelitis and the role of biofilms in chronic infection. FEMS Immunol Med Microbiol. 2008; 52:13–22. [PubMed: 18081847]

Chang DW, Nudell YA, Lau J, Zakharian E, Balashova NV. RTX Toxin Plays a Key Role in Kingella kingae Virulence in an Infant Rat Model. Infect Immun. 2014; 82:2318–2328. [PubMed: 24664507]

Chometon S, Benito Y, Chaker M, et al. Specific real-time polymerase chain reaction places Kingella kingae as the most common cause of osteoarticular infections in young children. Pediatr Infect Dis J. 2007; 26:377–381. [PubMed: 17468645]

Fine DH, Furgang D, Schreiner HC, et al. Phenotypic variation in Actinobacillus actinomycetemcomitans during laboratory growth: implications for virulence. Microbiology. 1999; 145:1335–1347. [PubMed: 10411260]

Foster MA, Walls T. High rates of complications following Kingella kingae infective endocarditis in children: a case series and review of the literature. Pediatr Infect Dis J. 2014; 33:785–786. [PubMed: 24921624]

Frye SA, Nilsen M, Tonjum T, Ambur OH. Dialects of the DNA uptake sequence in Neisseriaceae. PLoS Genet. 2013; 9:e1003458. [PubMed: 23637627]

Gene A, Garcia-Garcia JJ, Sala P, Sierra M, Huguet R. Enhanced culture detection of Kingella kingae, a pathogen of increasing clinical importance in pediatrics. Pediatr Infect Dis J. 2004; 23:886–888. [PubMed: 15361737]

Henriksen SD. "Pitting" and "corrosion" of the surface of agar cultures by colonies of some bacteria from the respiratory tract. Acta Pathol Microbiol Scand B Microbiol Immunol. 1974; 82:48–52. [PubMed: 4208333]

Ilharreborde B, Bidet P, Lorrot M, et al. New real-time PCR-based method for Kingella kingae DNA detection: application to samples collected from 89 children with acute arthritis. J Clin Microbiol. 2009; 47:1837–1841. [PubMed: 19369442]

Izano EA, Amarante MA, Kher WB, Kaplan JB. Differential roles of poly-N-acetylglucosamine surface polysaccharide and extracellular DNA in Staphylococcus aureus and Staphylococcus epidermidis biofilms. Appl Environ Microbiol. 2008; 74:470–476. [PubMed: 18039822]

Jakubovics NS, Grant Burgess J. Extracellular DNA in oral microbial biofilms. Microbes Infect. 2015; 7:531–537.

Kachlany SC, Planet PJ, Desalle R, Fine DH, Figurski DH, Kaplan JB. flp-1, the first representative of a new pilin gene subfamily, is required for non-specific adherence of Actinobacillus actinomycetemcomitans. Mol Microbiol. 2001; 40:542–554. [PubMed: 11359562]

Kaplan JB, Lo C, Xie G, et al. Genome sequence of Kingella kingae septic arthritis isolate PYKK081. J Bacteriol. 2012; 194:3017. [PubMed: 22582375]

Kaplan JB, Mulks MH. Biofilm formation is prevalent among field isolates of Actinobacillus pleuropneumoniae. Vet Microbiol. 2005; 108:89–94. [PubMed: 15917136]

Kehl-Fie TE, Miller SE, St Geme JW 3rd. Kingella kingae expresses type IV pili that mediate adherence to respiratory epithelial and synovial cells. J Bacteriol. 2008; 190:7157–7163. [PubMed: 18757541]

Kehl-Fie TE, Porsch EA, Miller SE, St Geme JW 3rd. Expression of Kingella kingae type IV pili is regulated by sigma54, PilS, and PilR. J Bacteriol. 2009; 191:4976–4986. [PubMed: 19465661]

Kehl-Fie TE, Porsch EA, Yagupsky P, et al. Examination of type IV pilus expression and pilus-associated phenotypes in Kingella kingae clinical isolates. Infect Immun. 2010; 78:1692–1699. [PubMed: 20145101]

Kehl-Fie TE, St Geme JW 3rd. Identification and characterization of an RTX toxin in the emerging pathogen Kingella kingae. J Bacteriol. 2007; 189:430–436. [PubMed: 17098895]

Kiedrowski MR, Kavanaugh JS, Malone CL, et al. Nuclease modulates biofilm formation in community-associated methicillin-resistant Staphylococcus aureus. PLoS One. 2011; 6:e26714. [PubMed: 22096493]

Kraus SJ, Glassman LH. Scanning electron microscope study of Neisseria gonorrhoeae. Appl Microbiol. 1974; 27:584–592. [PubMed: 4207582]

Kyme P, Dillon B, Iredell J. Phase variation in Bartonella henselae. Microbiology. 2003; 149:621–629. [PubMed: 12634331]

Lappann M, Claus H, van Alen T, et al. A dual role of extracellular DNA during biofilm formation of Neisseria meningitidis. Mol Microbiol. 2010; 75:1355–1371. [PubMed: 20180907]

Lequette Y, Boels G, Clarisse M, Faille C. Using enzymes to remove biofilms of bacterial isolates sampled in the food-industry. Biofouling. 2010; 26:421–431. [PubMed: 20198521]

Lynch AS, Robertson GT. Bacterial and fungal biofilm infections. Annu Rev Med. 2008; 59:415–428. [PubMed: 17937586]

Maldonado R, Wei R, Kachlany SC, Kazi M, Balashova NV. Cytotoxic effects of Kingella kingae outer membrane vesicles on human cells. Microb Pathog. 2011; 51:22–30. [PubMed: 21443941]

Marti S, Rodriguez-Bano J, Catel-Ferreira M, et al. Biofilm formation at the solid-liquid and air-liquid interfaces by Acinetobacter species. BMC Res Notes. 2011; 4:5. [PubMed: 21223561]

Mattick JS. Type IV pili and twitching motility. Annu Rev Microbiol. 2002; 56:289–314. [PubMed: 12142488]

Merritt JH, Kadouri DE, O'Toole GA. Growing and analyzing static biofilms. Curr Protoc Microbiol. 2005; Chapter 1(Unit 1B):1.

Montanaro L, Poggi A, Visai L, et al. Extracellular DNA in biofilms. Int J Artif Organs. 2011; 34:824–831. [PubMed: 22094562]

Parsek MR, Singh PK. Bacterial biofilms: an emerging link to disease pathogenesis. Annu Rev Microbiol. 2003; 57:677–701. [PubMed: 14527295]

Ravaioli S, Campoccia D, Visai L, et al. Biofilm extracellular-DNA in 55 Staphylococcus epidermidis clinical isolates from implant infections. Int J Artif Organs. 2011; 34:840–846. [PubMed: 22094564]

Rendueles O, Kaplan JB, Ghigo JM. Antibiofilm polysaccharides. Environ Microbiol. 2013; 15:334–346. [PubMed: 22730907]

Sheets AJ, Grass SA, Miller SE, St Geme JW 3rd. Identification of a novel trimeric autotransporter adhesin in the cryptic genospecies of Haemophilus. J Bacteriol. 2008; 190:4313–4320. [PubMed: 18424521]

Shirtliff ME, Mader JT. Acute septic arthritis. Clin Microbiol Rev. 2002; 15:527–544. [PubMed: 12364368]

Steichen CT, Cho C, Shao JQ, Apicella MA. The Neisseria gonorrhoeae biofilm matrix contains DNA, and an endogenous nuclease controls its incorporation. Infect Immun. 2011; 79:1504–1511. [PubMed: 21300774]

Wu J, Xi C. Evaluation of different methods for extracting extracellular DNA from the biofilm matrix. Appl Environ Microbiol. 2009; 75:5390–5395. [PubMed: 19561191]

Yagupsky P. Kingella kingae: carriage, transmission, and disease. Clin Microbiol Rev. 2015; 28:54–79. [PubMed: 25567222]

Yi K, Rasmussen AW, Gudlavalleti SK, Stephens DS, Stojiljkovic I. Biofilm formation by Neisseria meningitidis. Infect Immun. 2004; 72:6132–6138. [PubMed: 15385518]

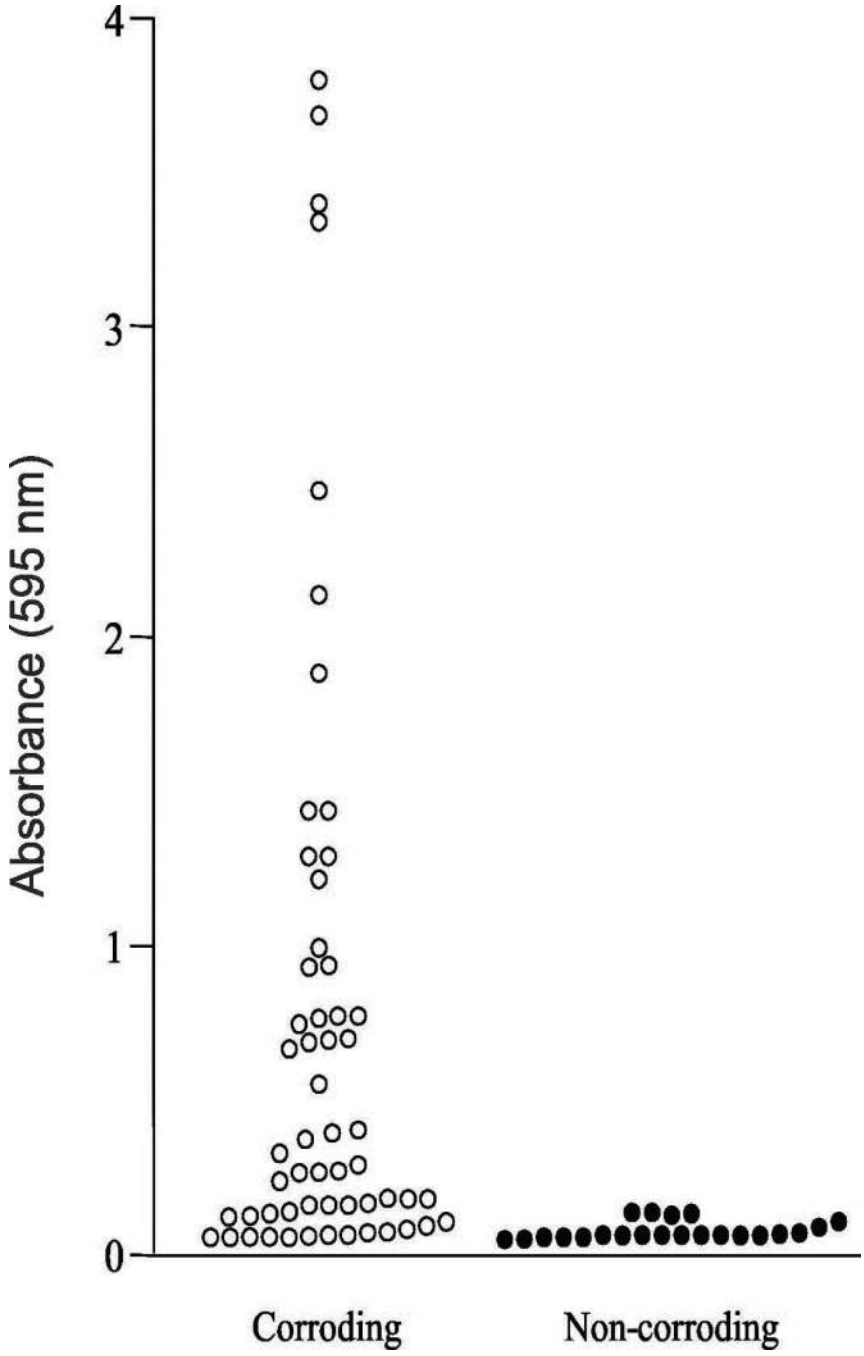

Fig. 1.

Biofilm formation by 58 corroding and 21 noncorroding *K. kingae* strains in 96-well microtiter plates. Biofilm was quantitated using a crystal violet binding assay. Absorbance at 595 nm is proportional to biofilm biomass.

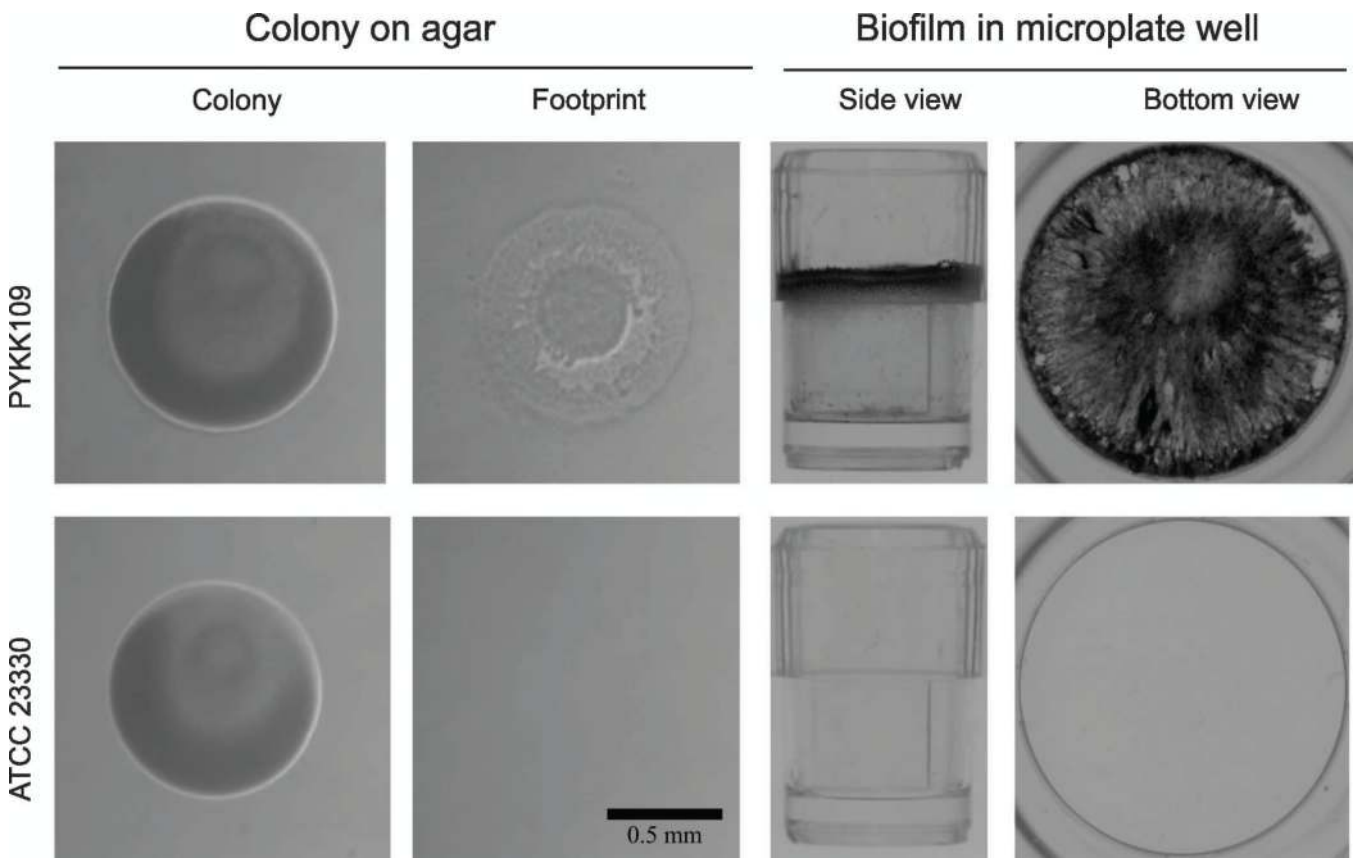

Fig. 2.

Colony morphologies on agar and biofilm phenotypes in broth of *K. kingae* corroding strain PYKK109 (top panels) and noncorroding strain ATCC 23330 (bottom panels). From left to right: bacterial colonies on agar; the agar surface beneath the colony after the colony was removed by rinsing with water; biofilm phenotype in broth (side view); biofilm phenotype in broth (bottom view).

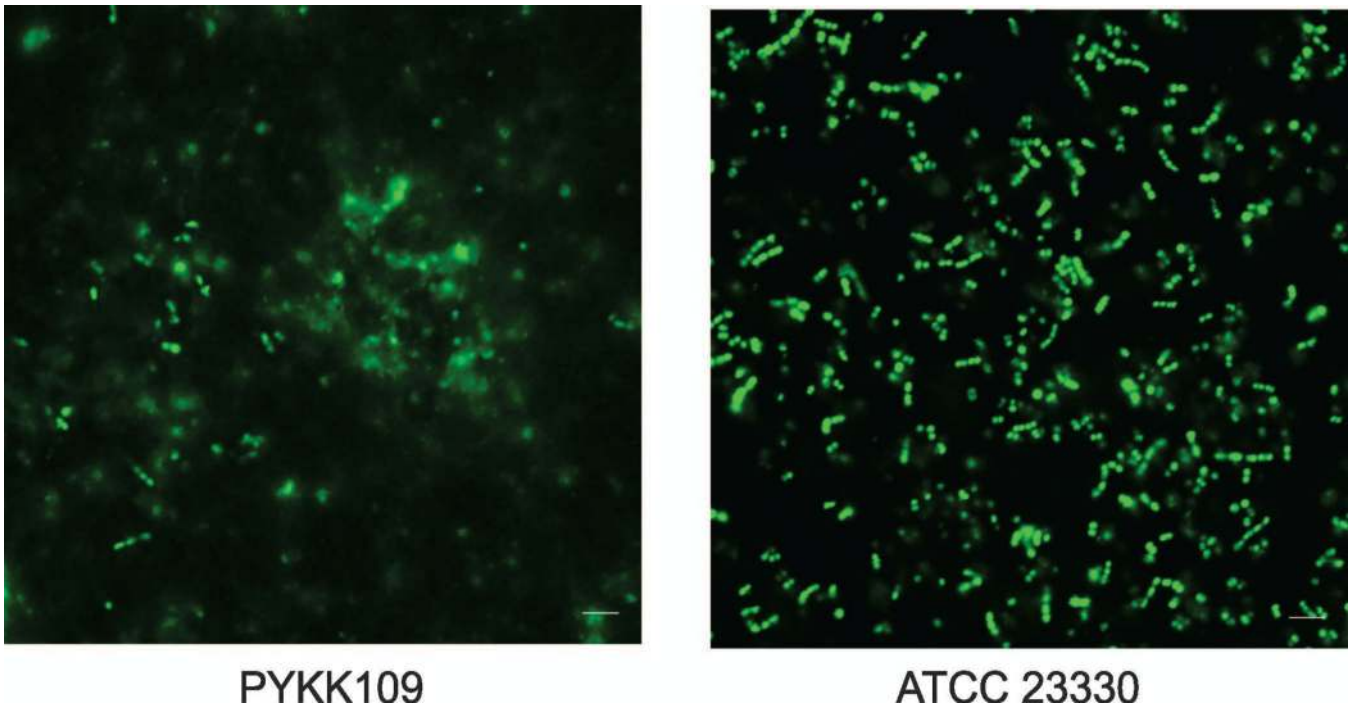

Fig. 3.

Confocal images of *K. kingae* bacterial cultures. The bacteria were grown in ibiTreat 60 μ-dishes plates for 24 h and then bacterial cultures were stained with 5 μM Sytox for 5 min at room temperature. The mages demonstrate extensive extracellular production of DNA by strain PYKK109 (Left panel) in contrast to strain ATCC 23330 (Right panel). Representative images are shown and are the results of three independent experiments. Scale bar =5μm.

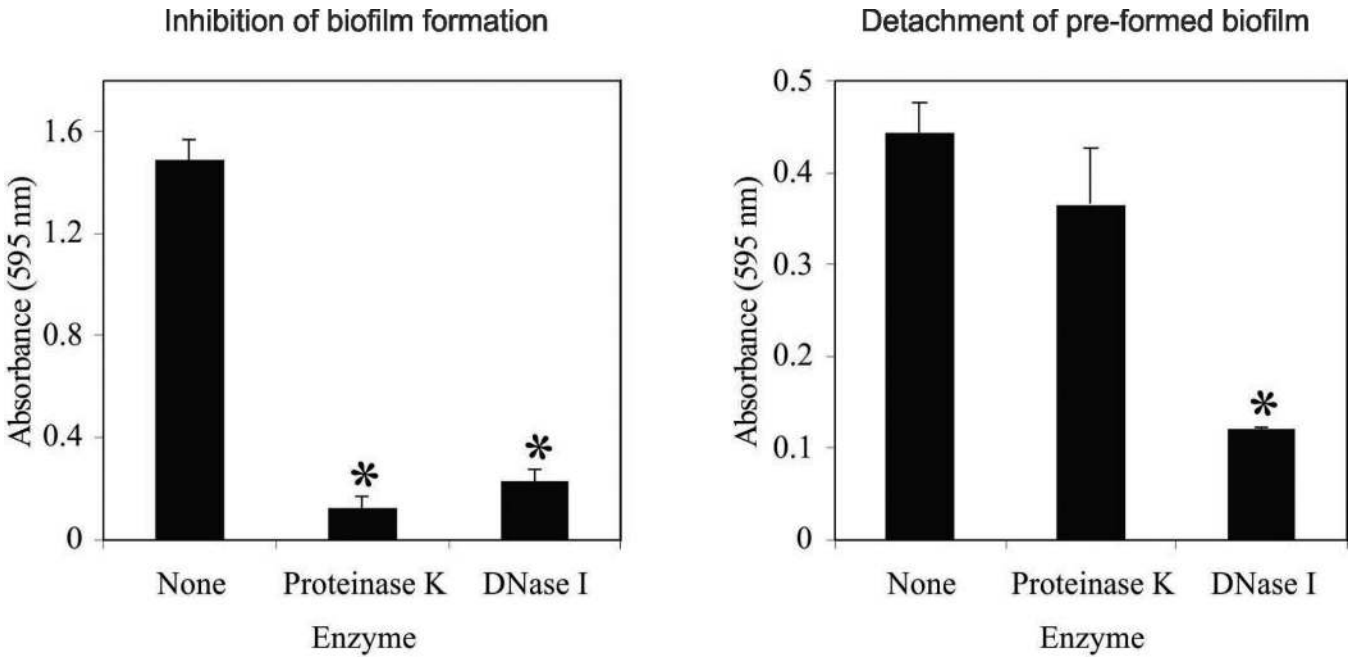

Fig. 4.

Effects of proteinase K and DNase I on *K. kingae* biofilm formation. In the left-hand graph, the enzymes were added to the broth at the time of inoculation and biofilm was quantitated after 24 h. In the right-hand graph, biofilms were cultured for 24 h and then treated with enzymes for 1 h. A_{595} values are proportional to biofilm biomass. Asterisks indicate values significantly different from no-enzyme controls ($P < 0.05$).

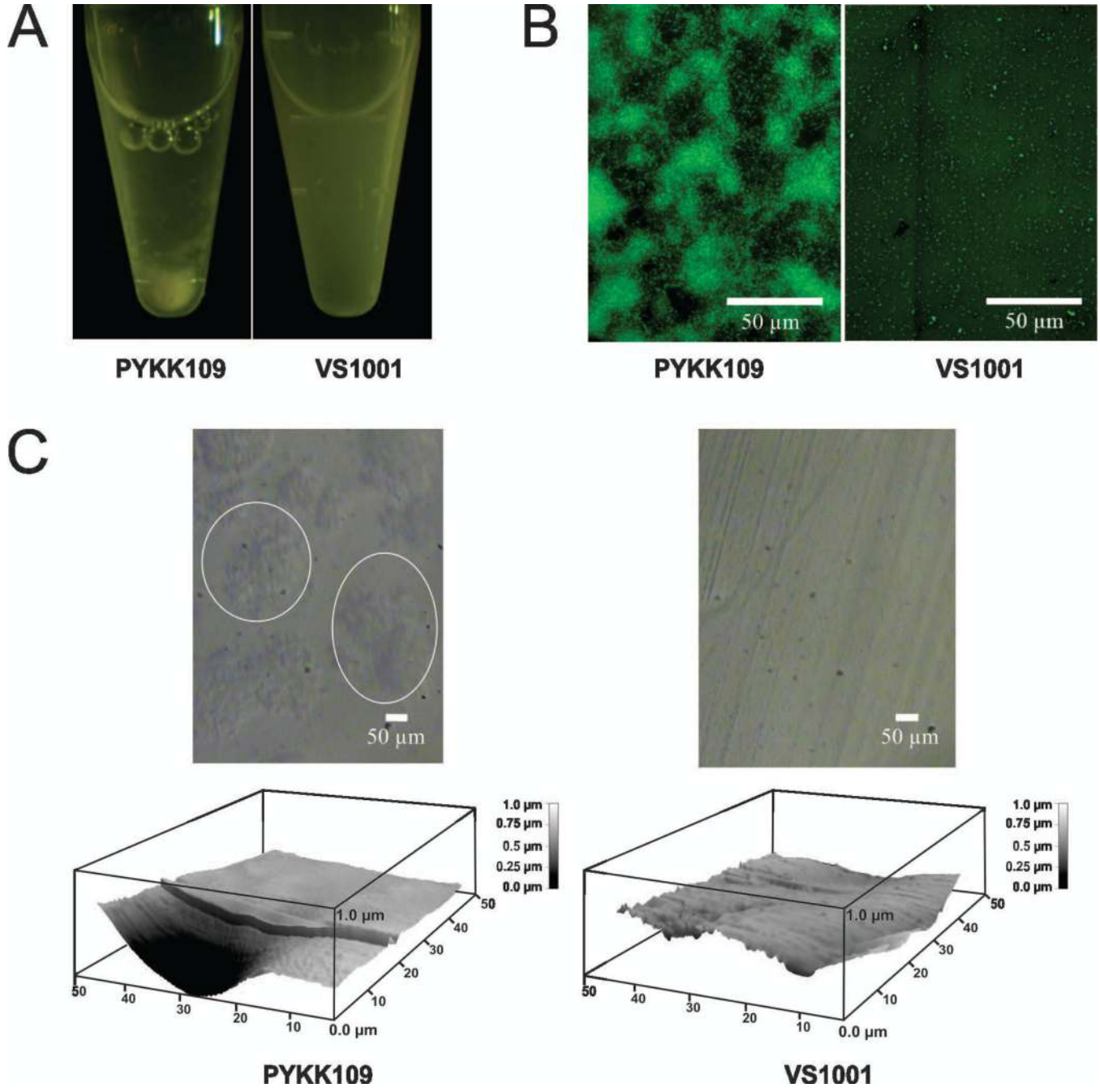

Fig. 5.

Autoaggregation, biofilm formation, and agar corrosion by *K. kingae* wild-type strain PYKK109 and pilus mutant strain VS1001. (A) Autoaggregation of cells in microcentrifuge tubes. (B) Biofilm formation on glass slides. In panel B, biofilms were visualized by staining with the green fluorescent nucleic acid stain SYTO9. (C) AFM topographic image (top) and cross-sectional profile (bottom) of agar surface after the bacteria were washed from the agar surfaces. For the pitted sample, the free amplitude and setpoint were 156 nm and 83 nm, respectively. For the control sample, those values were 208 nm and 145 nm. Areas of agar depression are designated with white circles.

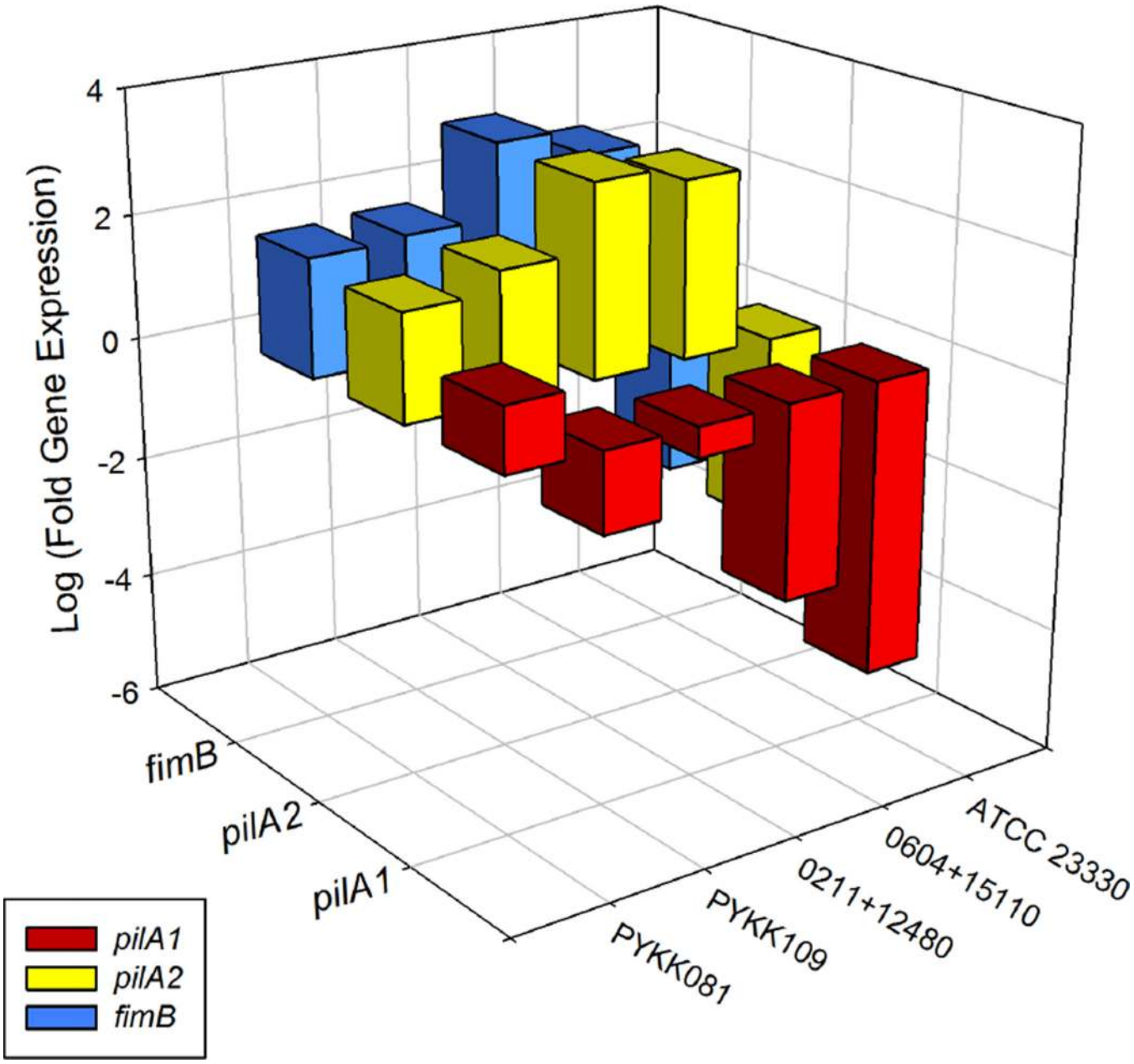

Fig. 6.

Transcript levels of genes *pilA1, pilA2, fimB* for type IV pili production in biofilm-forming strains PYKK081, PYKK109, 0211+12480 and non-biofilm forming strains ATCC 23330, 0604+15110. Transcripts levels are expressed relative to glyceraldehyde 3-phosphate dehydrogenase (GAPDH), SEM ≥5%.

Table 1

PYKK109 biofilm composition

Macromolecule quantities (protein, carbohydrate, and DNA) were measured in PYKK109 biofilms as described in Methods and were expressed as μg of mass per cm^2 surface area. The experiment was repeated three independent times, each experimental condition was performed in triplicates. Average results ± SEM are displayed.

Molecule	Total biofilms	Extracellular biofilm matrix
Total carbohydrates	25 ± 4.30	0.4 ± 0.05
Protein	3250 ± 11.80	490 ± 0.55
DNA	0.79 ± 0.10	0.68 ± 0.08
DNA/nuclease treated	0.10 ± 0.04	0.06 ± 0.05